Magnetic Resonance Imaging 52 (2018) 16–23

Contents lists available at ScienceDirect

Magnetic Resonance Imaging

journal homepage: www.elsevier.com/locate/mri

Technical note

Accuracy and precision of quantitative DCE-MRI parameters: How should one estimate contrast concentration?☆

Nicole Wake[a,b,*], Hersh Chandarana[a,b], Henry Rusinek[a], Koji Fujimoto[c], Linda Moy[a], Daniel K. Sodickson[a,b], Sungheon Gene Kim[a,b]

[a] Center for Advanced Imaging Innovation and Research (CAI2R), Bernard and Irene Schwartz Center for Biomedical Imaging, Department of Radiology, NYU School of Medicine, New York, NY, United States
[b] Sackler Institute of Graduate Biomedical Sciences, NYU School of Medicine, New York, NY, United States
[c] Department of Diagnostic Imaging and Nuclear Medicine, Kyoto University, Kyoto, Japan

ARTICLE INFO

Keywords:
Dynamic contrast-enhanced MRI
Perfusion
Pharmacokinetic model
Contrast agent concentration

ABSTRACT

Introduction: Pharmacokinetic parameters derived from dynamic contrast-enhanced MRI (DCE-MRI) data are sensitive to acquisition and post-processing techniques, which makes it difficult to compare results obtained using different methods. In particular, one of the most important factors affecting estimation of model parameters is how to convert MRI signal intensities to contrast agent concentration. The purpose of our study was to quantitatively compare a linear signal-to-concentration conversion (LC) as an approximation and a non-linear conversion (NLC) based on the MRI signal equation, in terms of the accuracy and precision of the pharmacokinetic parameters in T_1-weighted DCE-MRI.

Materials and methods: Numerical simulation studies were conducted to compare LC and NLC in terms of the accuracy and precision in contrast kinetic parameter estimation, and to evaluate their dependency on flip angle (FA), pre-contrast T_1 (T_{10}) and arterial input function (AIF). In addition, the effect of the conversion method on the diagnostic accuracy was evaluated with 36 breast lesions (19 benign and 17 malignant).

Results: The transfer rate (K^{trans}) estimated using LC and measured AIF (mAIF) were up to 38% higher than the true K^{trans} values, while the LC K^{trans} estimates with the presumed AIF (pAIF) were up to 7% lower than the true K^{trans} values, when FA = 45°. When using a small FA, such as 12°, the LC K^{trans} with pAIF had least sensitivity to the error in T_{10} compared to the K^{trans} estimated using LC with mAIF, and NLC with pAIF or mAIF. The breast DCE-MRI study showed that both LC and NLC K^{trans} were significantly different ($p < 0.05$) between the malignant and benign lesions. The effect size between benign and malignant values as measured by Cohen's d was 1.06 for LC K^{trans} and 1.02 for NLC K^{trans}.

Conclusion: The present study results show that, when precontrast T_1 measurement is not available and a low FA is used for DCE-MRI, the uncertainty in the contrast kinetic parameter estimation can be reduced by using the LC method with pAIF, without compromising the diagnostic accuracy.

1. Introduction

T_1-weighted dynamic contrast-enhanced magnetic resonance imaging (DCE-MRI) has been used for quantitative measurement of the tumor microcirculation environment [1–6]. DCE-MRI data are often used to estimate contrast kinetic model parameters, such as the volume transfer constant (K^{trans}), the extracellular volume fraction (v_e), and the exchange rate constant K_{ep} (K^{trans}/v_e), as tumor biomarkers [2,7–11]. However, due to measurement variability, it remains challenging to compare contrast kinetic parameters from different DCE-MRI studies [12,13]. One of the major factors that influences the contrast kinetic parameters is conversion of MRI signal to the concentration of contrast agent (CA). The relationship between signal and CA concentration depends on MRI scan parameters, such as flip angle (FA) and repetition time (TR), as well as pre-contrast longitudinal relaxation time T_1 (T_{10}) [14–16].

Most routine clinical DCE-MRI exams do not include actual FA or T_1 measurements, because it is not trivial to perform accurate B_1 and T_1 mapping of a large volume of interest in a relatively short time. In the absence of measured FA (i.e., B1+ field inhomogeneity) and T_{10} values,

☆ Funding: This work was supported by the National Institute of Health [grant numbers NIH R01CA160620 and NIH P41 EB017183].
* Corresponding author at: 660 First Avenue, 4th Floor, New York, NY 10016, United States.
E-mail address: nicole.wake@nyumc.org (N. Wake).

https://doi.org/10.1016/j.mri.2018.05.007
Received 7 February 2018; Received in revised form 14 May 2018; Accepted 15 May 2018

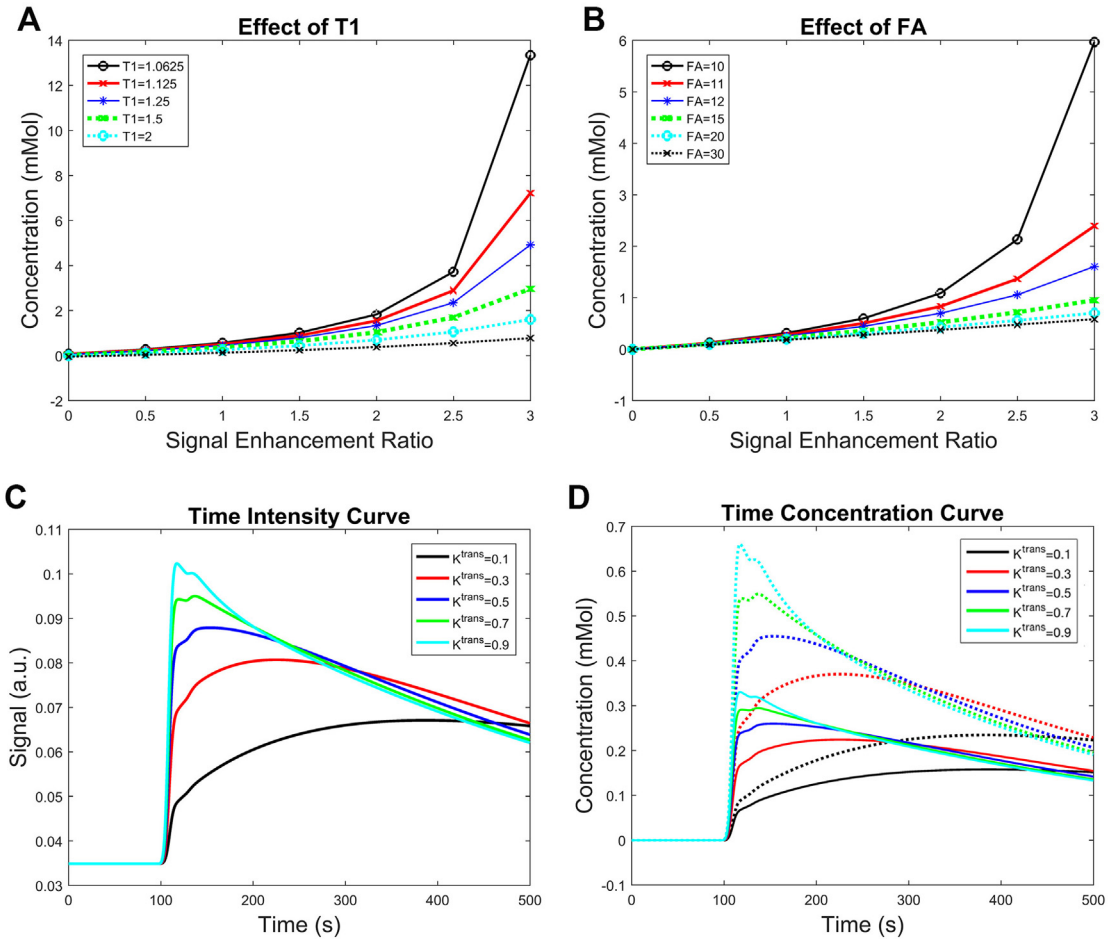

Fig. 1. Effect of (A) T1 and (B) FA on signal enhancement ratios and concentration for NLC method. (C) Lesion signal enhancement curve (D) lesion time concentration curve (solid line = LC, dashed line = NLC).

particularly in clinical scans, the DCE-MRI data are converted to the concentration values using the assumption of linearity between signal enhancement and concentration. In computed tomography, it is valid to assume a linear relationship between Hounsfield Units and iodine concentration [17,18]. It is also reasonable to do so in other nuclear medicine imaging modalities, such as single-photon emission computed tomography and positron emission tomography, where the signal is measured from the tracers directly. However, in MRI, the relationship between signal intensity and CA concentration approaches linearity only for a low concentration level and limited range of image acquisition parameters [15,19].

Although it is generally known that the differences in signal conversion methods can affect pharmacokinetic parameter estimations, the effect of these conversions on the estimation of pharmacokinetic model parameters has not been studied in a wide range of contrast kinetic values and scan parameters. Heilmann et al. [20] demonstrated that the application of a linear approach led to inaccurate estimates of kinetic parameters including K^{ep}. In contrast, a recent study with 17 patients showed that linear conversion may be acceptable for quantification of model-free hepatic perfusion parameters when a relatively large FA of 45° was used [21]. Further comprehensive study on the effect of signal-to-concentration conversion method can be helpful in comparing DCE-MRI studies with different scan parameters and assumptions in data analysis.

Hence, the purpose of our study was to compare linear signal intensity-to-concentration conversion (LC) and non-linear conversion (NLC) methods in terms of the accuracy and precision in contrast kinetic parameter estimation, and to evaluate their dependency on the image acquisition parameters such as FA and T_{10}. In addition, we sought to evaluate the effect of including the arterial input function (AIF) in the conversion process as in when the AIF is measured, as opposed to the case of not-including the AIF for the conversion when the AIF is assumed to be known, for instance using a population-based AIF already defined in concentration. Finally, we investigated the effect of the signal-to-concentration conversion method on pharmacokinetic parameters derived on malignant and benign lesions for breast DCE-MRI exams.

2. Methods

2.1. Signal to concentration conversion

In this study, we consider two methods, LC and NLC, to convert T_1-weighted MRI signal intensity S(t) to CA concentration C(t). For the LC method, the conversion was performed assuming a linear relationship between the S(t) and C(t):

$$C(t) = \frac{1}{r_1 T_{10}} \left(\frac{S(t)}{S_0} - 1 \right) \quad (1)$$

where S_0 is the average pre-contrast signal level, r_1 is the longitudinal relaxivity, and T_{10} is the tissue or blood T_1 before CA injection [6,22].

For the NLC method, we assume the data acquisition is conducted with a spoiled gradient echo sequence (SPGR). The signal equation of SPGR includes the imaging parameters (TR and FA = α) and T_{10} of the tissue of interest [23]. In the NLC method, the CA concentration is estimated using the following equation, in the fast water exchange limit

regime:

$$C(t) = \frac{1}{r_1}\cdot\left(\frac{1}{T_1(t)} - \frac{1}{T_{10}}\right) \quad (2)$$

where $T_1(t)$ can be directly derived using the SPGR signal equation:

$$S(t) = M_0\frac{1 - \exp\left(-\frac{TR}{T_1(t)}\right)}{1 - \cos(\alpha)\cdot\exp\left(-\frac{TR}{T_1(t)}\right)}\sin(\alpha) \quad (3)$$

where M_0 is the fully relaxed signal for a 90° pulse when $TR \gg T_{10}$. It is assumed that TE is short enough such that the T_2^* effect is negligible. The complex transverse magnetization signal measured in MRI can be described as

$$S_n(t) = (S_x(t) + n_x) + i(S_y(t) + n_y) \quad (4)$$

where $S_x(t)$ and $S_y(t)$ are the x and y- component of S(t) in the transverse plane, and n_x and n_y are the measurement noise. The magnitude of $S_n(t)$, $|S_n(t)|$, is typically used for DCE-MRI data analysis. Although $|S_n(t)|$ includes noise as in Eq. (4), Eq. (3) is often used to estimate $T_1(t)$ by assuming $S(t) \sim |S_n(t)|$:

$$T_1(t) = \frac{-TR}{\ln\left(A - \frac{|S(t)|}{S_0}\right) - \ln\left(A - \frac{|S(t)|}{S_0}\cos(\alpha)\right)} \quad (5)$$

where $A = (1 - \cos(\alpha)e^{-TR})/(1 - e^{-TR})$. The degree of non-linearity of the NLC method, Eqs. (2)–(5)., depends on tissue T_{10} and FA as shown in Fig. 1A and B, respectively, when noise is negligible. The error introduced by the assumption of negligible noise in this conversion is then nonlinearly propagated to estimation of CA concentration using Eq. (2). Note that the same assumption is used for the LC method in Eq. (1) where the noise introduced in S(t) is linearly propagated to C(t). In this study, we assessed how the noise affects estimation of contrast kinetic parameters when using LC and NLC methods, in addition to the main focus of this study to assess the effect of T1 and flip angle in the LC and NLC methods.

The difference between these two conversion methods is evaluated in terms of contrast kinetic model parameters. For this purpose, we used the generalized kinetic model (GKM), also known as the Tofts model, which is one of the simplest and most widely used contrast kinetic models. GKM is expressed as

$$C(t) = K^{trans}\int_0^t C_p(u)\exp(K^{trans}(t - u)/v_e)du \quad (6)$$

where $C_p(t)$ is the contrast concentration in the plasma, K^{trans} the volume transfer coefficient reflecting vascular permeability and plasma flow, and v_e the extravascular extracellular space volume fraction [13]. Both K^{trans} and v_e were estimated by fitting the GKM to the measured data:

$$\{K^{trans}, v_e\} = \arg\ \min \sum_t (C_m(t) - C(t))^2 \quad (7)$$

where $C_m(t)$ is the measured contrast concentration and C(t) is the predicted contrast concentration by Eq. (6). Fitting was performed using the Nelder-Mead simplex method [24], a multi-dimensional unconstrained nonlinear minimization, provided in Matlab (The Mathworks, Inc., Natick, MA), with maximum number of iterations = 3000 and termination tolerance on the cost function value and parameter = $1e^{-4}$.

Numerical simulation of DCE-MRI data and contrast kinetic analysis were performed using either a presumed AIF (pAIF) that is defined in concentration or a measured AIF (mAIF) that is converted to concentration using the LC or NLC method along with the tissue signal. The population based AIF by Parker et al. [25] was used as the pAIF. For the simulation study, the mAIF was generated by converting the pAIF to S(t) using Eqs. (2) and (3), adding noise, and then reconverting it back to $C_p(t)$ such that the AIF would have the effect of noise in measurement as well as signal-to-concentration conversion. Fig. 1C shows the time intensity curves S(t) generated using Eqs. (2)–(4). with $K^{trans} = 0.1$–$0.9\ min^{-1}$, $v_e = 0.5$, TR = 6.8 ms, and FA = 12°. Fig. 1D demonstrates that the CA concentration curves estimated from the LC and NLC methods show substantial differences from each other. In this study, we systematically investigated the differences between these two methods in terms of the estimated GKM parameters.

2.2. Simulation studies

Numerical simulations were carried out to investigate: 1) the uncertainty in contrast kinetic parameter estimation, 2) the effect of FA, and 3) the effect of assumed T_{10} on the LC and NLC methods. S(t) was generated using Eqs. (2)–(4). with a range of tissue conditions and scan protocol depending on the goal of each simulation study as described below. Realistic signal with Rician noise, $S_n(t)$, was generated using the following:

$$S_n(t) = \sqrt{(S(t) + n_r)^2 + (n_i)^2} \quad (8)$$

where n_r and n_i are Gaussian random noise with zero mean and standard deviation corresponding to 10% of the average pre-contrast signals. The temporal resolution was kept at 1 s/frame in order to avoid any influence from a low temporal resolution. The total scan time was 8.3 min with 1.3 min of pre-contrast scan. For each simulation condition, the signal with noise, $S_n(t)$, was generated 20 times in order to measure the range of estimated GKM parameters.

Once $S_n(t)$ was generated, it was converted to CA concentration curves C(t) using either the LC or NLC method. Then, the GKM model (Eq. (4)) was fit to the C(t) generated from both methods, with random initial values. The higher the FA, the more linear the relationship between S(t) and $1/T_1 = R_1$ is as shown in Fig. 1, while the sensitivity of perfusion sequences is higher with a smaller FA [15]. FA = 45° was used as an example of high FA that gives a near-linear relationship between SI and R_1, and FA = 12° as an example of low FA cases that are commonly used in clinical DCE-MRI exams [21,26,27]. T_{10} was assumed to be 1660 ms for the arterial blood and 1500 ms for the lesion [21,28–30]. $r_1 = 3.9\ Lmmol^{-1}\ s^{-1}$ was used for all simulations. All simulation studies were conducted using the pAIF as well as the mAIF in order to investigate the effect of including AIF in signal-to-concentration conversion.

Simulation study 1: To assess the effect of LC and NLC on the uncertainty in contrast kinetic parameter estimation. K^{trans} was varied from 0.1 to $0.9\ min^{-1}$ while v_e was fixed to 0.3. While keeping K^{trans} constant at $0.5\ min^{-1}$, v_e was then varied from 0.1 to 0.5. For each pair of true K^{trans} and v_e values, K^{trans} and v_e were estimated. FA = 45° was used for this study.

Simulation study 2: To assess the effect of FA on the LC and NLC methods. This study was conducted using a pair of representative K^{trans} and v_e values ($K^{trans} = 0.5\ min^{-1}$ and $v_e = 0.3$). FA was varied from 7.5° to 85°. K^{trans} and v_e were estimated for each FA.

Simulation study 3: To assess the effect of the error in T_{10} on the LC and NLC methods. This study was conducted using $K^{trans} = 0.5\ min^{-1}$ and $v_e = 0.3$. DCE-MRI data were generated using T_{10} = 1500 ms for the lesion, while the data analysis of the lesion was conducted assuming the lesion T_{10} value to range from 700 ms and 2500 ms. K^{trans} and v_e were estimated for each presumed T_{10} value. This simulation study was repeated with FA = 12° and 45°.

2.3. Breast cancer study

DCE-MRI data from 32 patients with 36 breast lesions (19 benign, 17 malignant) were included in this study to investigate the effect of using the LC and NLC methods on differentiating malignant lesions from benign ones. Prior Institutional Review Board approval was

obtained for this retrospective analysis. All images were acquired on a whole-body 3 T scanner (MAGNETOM TimTrio, Siemens Healthcare, Erlangen, Germany) equipped with a seven element breast coil (InVivo, FL). DCE-MRI scans were conducted using a prototype radial stack-of-stars three-dimensional (3D) SPGR pulse sequence with golden-angle spoke ordering for continuous data acquisition before, during, and after contrast administration (0.1 mM/Kg body weight). Relevant imaging parameters were: sagittal slab orientation, field of view = 280 × 280 × 144 mm^3, FA = 12°, TE/TR = 1.47/3.6 ms, and bandwidth = 710 Hz/pixel. DCE-MRI images were reconstructed with a temporal resolution of 5 s/frame (34 spokes/frame) using the Golden-angle Radial Acquisition Sparse and Parallel (GRASP) MRI method [30,31]. Tumor regions of interest (ROIs) for all patients were drawn by a board-certified breast radiologist. The pAIF used for the simulation study was also used for the analysis of the patient data; and the kinetic parameters K^{trans} and v_e were estimated and compared for both LC and NLC methods.

2.4. Statistical analysis

The estimated contrast kinetic parameters obtained with different signal conversion methods were compared using an unpaired *t*-test at the two-sided 5% significance level. In addition, K^{trans} and v_e estimates were compared with the true values that were used to generate the DCE-MRI data and were used to determine the accuracy and precision of each method. Accuracy was measured as percent error defined as $(|\text{true value} - \text{estimated value}| / \text{true value}) * 100$ and precision was measured as the coefficient of variation defined as (standard deviation / mean value) * 100. All simulations and analyses were conducted using MatLab (The Mathworks Inc., Natick, MA).

3. Results

3.1. Simulation study

3.1.1. Simulation 1: uncertainty in parameter estimation

The goal of Simulation study 1 was to assess the uncertainty in contrast kinetic parameter estimation associated with the signal-to-concentration conversion method over a range of K^{trans} and v_e values (Fig. 2). In all cases, the NLC provided more accurate estimates of both K^{trans} and v_e than the LC method. The error with the NLC method was < 2% regardless of the AIF type (pAIF or mAIF). For the cases with a fixed v_e (0.3) and varying K^{trans} (0.1–0.9 min^{-1}) (Fig. 2A and B), the LC K^{trans} estimates with the mAIF were about 20–38% higher than the true K^{trans} values, while the LC K^{trans} estimates with the pAIF were about 3–7% lower than the true K^{trans} values. There were significant differences ($p < 0.05$) between all estimates made using the NLC and LC except for K^{trans} estimates made using the mAIF when $K^{trans} = 0.1\ min^{-1}$. The difference between the LC v_e estimates using the pAIF and mAIF was substantially smaller than that in the K^{trans}. For the cases with varying K^{trans} and fixed v_e, the precision ranged from 1.7% to 2.9%. K^{trans} estimates made using LC with mAIF were most precise (CV = 1.7%) and v_e estimates made using LC with pAIF were least precise (2.9%). There were significant differences ($p < 0.05$) in precision for K^{trans} estimates made with NLC and LC using the mAIF and LC with pAIF and mAIF.

For the cases with varying v_e (0.1–0.5) and a fixed K^{trans} (0.5 min^{-1}), the LC v_e estimates with the mAIF were about 1–8% higher than the true v_e values, while the LC v_e estimates with the pAIF was about 3–7% lower than the true v_e values (Fig. 2C and D). Precision for both LC and NLC methods using the pAIF and mAIF ranged from 1.9–3.2%. The LC K^{trans} estimates with the mAIF were up to about 40% higher than the true K^{trans} values although its precision was compatible with others. There were no significant differences in the precision of the measurements for these cases with fixed K^{trans} and varying v_e.

3.1.2. Simulation 2: effect of flip angle

In the second simulation study, the effect of FA was investigated using representative K^{trans} and v_e values (Fig. 3). When the pAIF was used, the NLC method provided accurate estimates of both K^{trans} and v_e for all FAs (error < 2.3%). The LC K^{trans} estimates were not significantly different from the true K^{trans} when FA > 75°. However, as FA decreased, the LC K^{trans} estimates decreased gradually, underestimating K^{trans} by up to 67% when FA = 7.5°. Similarly, the LC v_e estimates were not significantly different from the true v_e when FA > 65°, but the error increased gradually up to 55% as FA decreased to 7.5°. Precision for both the NLC and LC methods was within 2% for FA = 85°, and it increased to 8% and 5% with FA = 7.5° for the NLC and LC methods respectively.

When the mAIF was used, the NLC method provided accurate estimates (< 2% error) of K^{trans} and v_e for FAs ≥ 10°; and percent error increased to 7% for K^{trans} and 9% for v_e with FA = 7.5°. As FA decreased from 85° to 7.5°, the LC K^{trans} estimates increased gradually with an overestimation of 748% when FA = 7.5°. The LC v_e estimates were not significantly different from the true v_e when FA > 65°, but increased gradually overestimating v_e by as much as 54% as FA decreased to 7.5°. Precision for the NLC method ranged from 1.8–7% for K^{trans} and 2.2–4.7% for v_e estimates, and for the LC method precision ranged from 2.8–6.4% for K^{trans} and 2.2–3.7% for v_e estimates. There were no significant differences in any of the precision measurements for varying FA.

3.1.3. Simulation 3: effect of precontrast T_1

The effect of T_{10} was investigated in the third simulation study using the simulation data using $K^{trans} = 0.5\ min^{-1}$ and $v_e = 0.3$. When the correct T_{10} value (T_{10} = 1500 ms) was used, the NLC method accurately estimated K^{trans} and v_e (< 1% error) as expected. Overall, for both conversion methods, the error in the assumed T_{10} resulted in monotonical changes in the estimated K^{trans} and v_e; the higher the assumed T_{10} was, the lower the estimated K^{trans} and v_e (Fig. 4).

When FA = 12° and the assumed T_{10} varied from 0.7–2.5 s, the largest errors were seen in K^{trans} estimates made using the LC with the mAIF (K^{trans} = 5.32–1.46 min^{-1}) and the smallest errors were seen in K^{trans} estimates made using LC with the pAIF (K^{trans} = 0.61–0.17 min^{-1}). The NLC with the mAIF had the greatest variability in v_e, with v_e values ranging from 1.11 to 0.15, while the LC v_e with the pAIF showed the smallest changes in estimated v_e values (0.43–0.12). Hence, both K^{trans} and v_e estimates were least affected by the assumed T_{10} when the LC method was used with the pAIF (Fig. 4A and B).

When FA = 45° was used, the change in the estimated K^{trans} and v_e due to T_{10} was similar to that when FA = 12° among the four different methods (LC vs. NLC; pAIF vs. mAIF) (Fig. 4C and D). It was noted that the K^{trans} estimated using the LC method with the pAIF were closer to those using the NLC methods than the K^{trans} estimated using the LC method with the mAIF.

Precision measurements for all simulations ranged from 2.3–2.7% for FA = 45° and 0.3–2.6% using the FA = 12°. There were no significant differences in any of the precision measurements for varying T_{10} when FA = 45°. For FA = 12°, K^{trans} estimates made using the LC method with the pAIF were the most precise (0.3%) and v_e measurements made using NLC with mAIF were the least precise (2.6%). There were significant differences ($p < 0.05$) between all measurements except for K^{trans} and v_e measurements made using LC or NLC with the pAIF.

3.2. Breast cancer study

For the 32 patients with breast lesions, the contrast kinetic model analysis was conducted using the pAIF. K^{trans} estimates were 30–35% lower with LC than with NLC, and the v_e estimates were 60–65% lower using LC as compared to those using NLC (Fig. 5), which are consistent

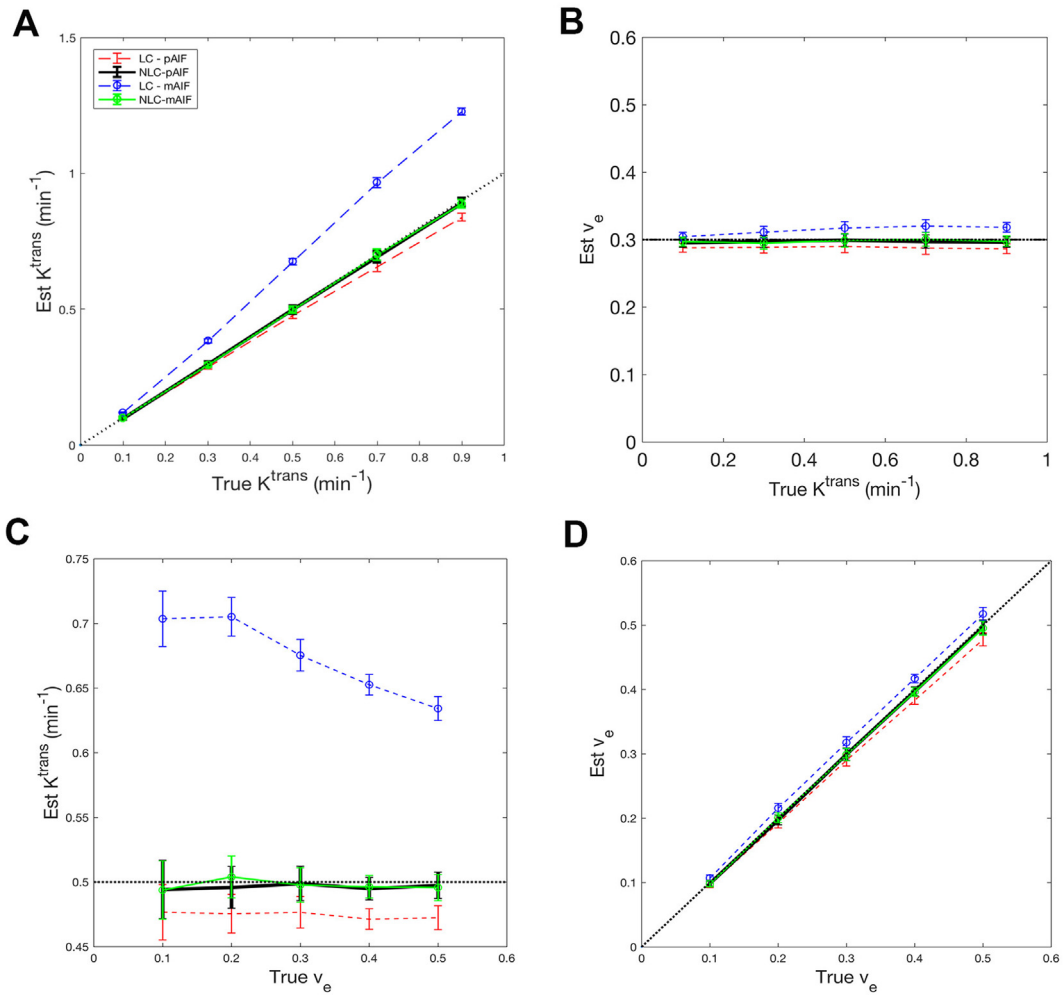

Fig. 2. K^{trans} and v_e estimates from concentration curves generated using the LC and NLC methods with the pAIF and mAIF. (A) K^{trans} and (B) v_e estimates for fixed v_e (0.3) and varying true K^{trans} (0.1–0.9 min^{-1}). (C) K^{trans} and (D) v_e estimates for fixed K^{trans} (0.5 min^{-1}) and varying v_e (0.1–0.5).

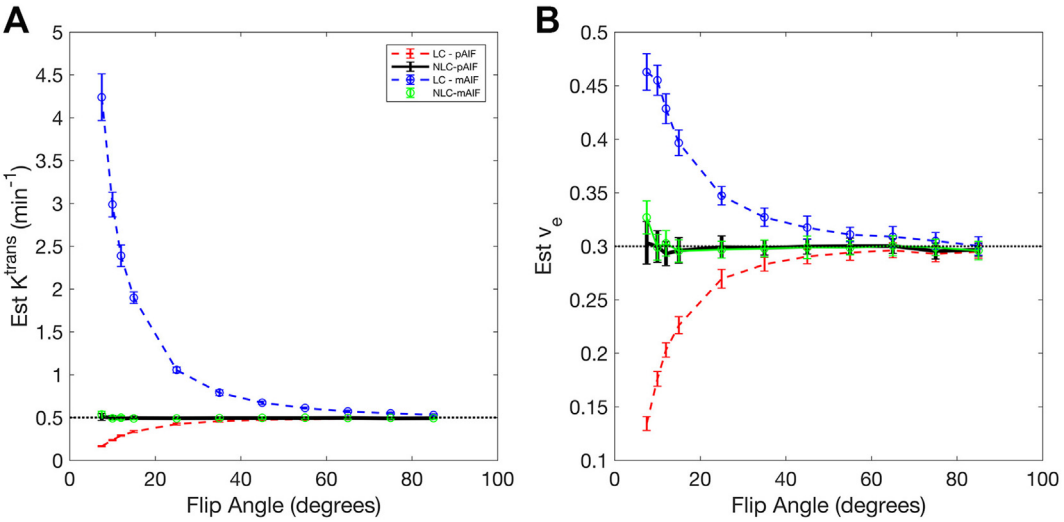

Fig. 3. Effect of FA used for data acquisition on estimation of K^{trans} and v_e using the LC and NLC methods. (True K^{trans} = 0.5 min^{-1}, True v_e = 0.3). (A) Estimated K^{trans} and (B) estimated v_e.

with the simulation results. A similar trend was observed with the parametric maps. Fig. 6 shows parametric maps for one representative patient using the NLC and LC methods. There was significant difference ($p < 0.05$) between the K^{trans} estimates of the patients with malignant and benign lesions, in the cases of both LC and NLC. The effect sizes between benign and malignant values as measured by Cohen's d were 1.06 for LC K^{trans}, 1.02 for NLC K^{trans}, 0.26 for LC v_e, and 0.45 for NLC v_e.

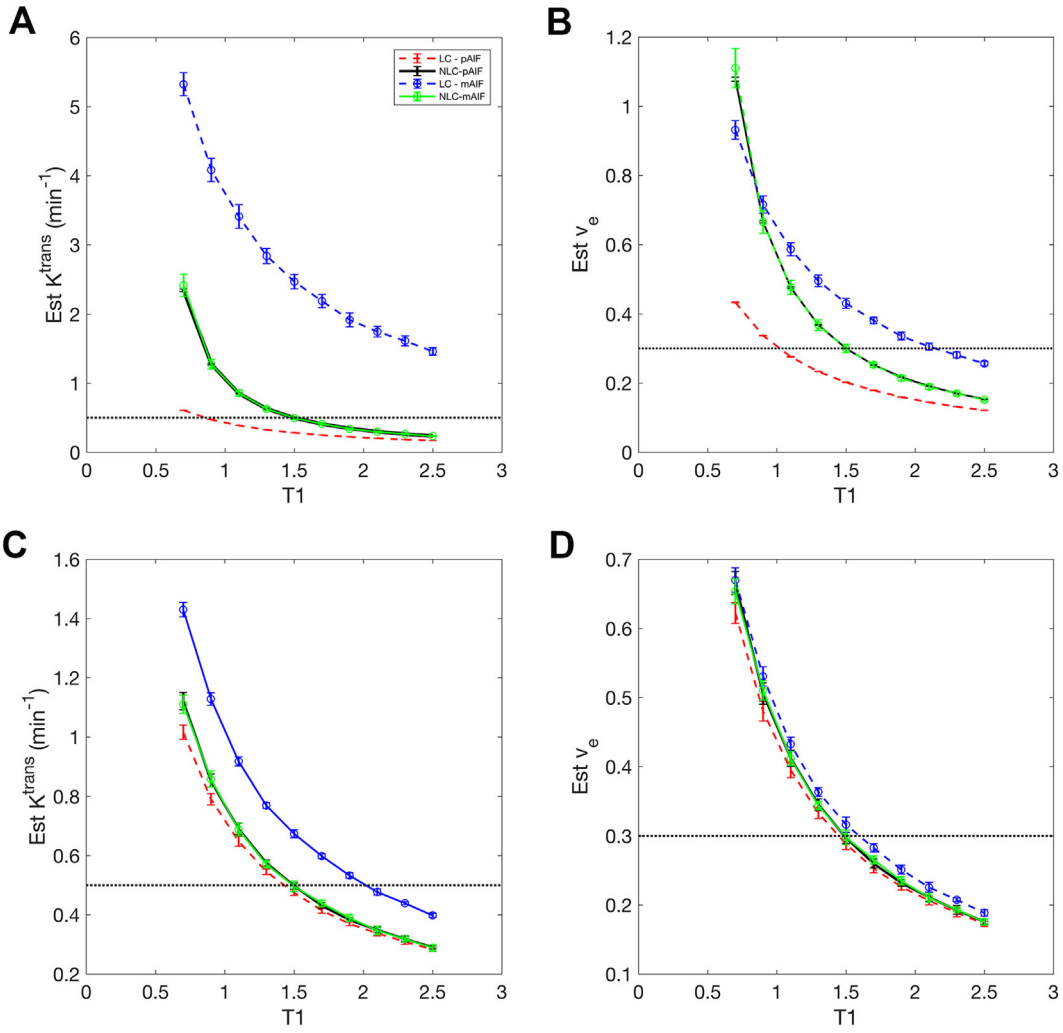

Fig. 4. Effect of incorrect tissue T1 values on K^{trans} and v_e estimates using the LC and NLC methods. (A) Estimated K^{trans} and (B) Estimated v_e using a 12° FA (C) estimated K^{trans} and (D) estimated v_e using a 45° FA.

4. Discussion

Conversion of T_1-weighted DCE-MRI data to CA concentration is one of the important steps for accurate estimation of pharmacokinetic parameters. Among many factors that can affect the signal-to-concentration conversion, we investigated how the accuracy and precision of K^{trans} and v_e were affected using a LC method in comparison to a NLC method based on the theoretical signal equation of SPGR pulse sequence commonly used for DCE-MRI exams. Overall, our simulation data shows that both K^{trans} and v_e estimates using LC were overestimated as compared to those using NLC when the mAIF was used, while both K^{trans} and v_e using LC with the pAIF were underestimated. These findings are consistent with the earlier studies that showed the assumption of signal linearity may result in miscalculations of pharmacokinetic parameters [20,21].

The results in this study also demonstrate that the parameter

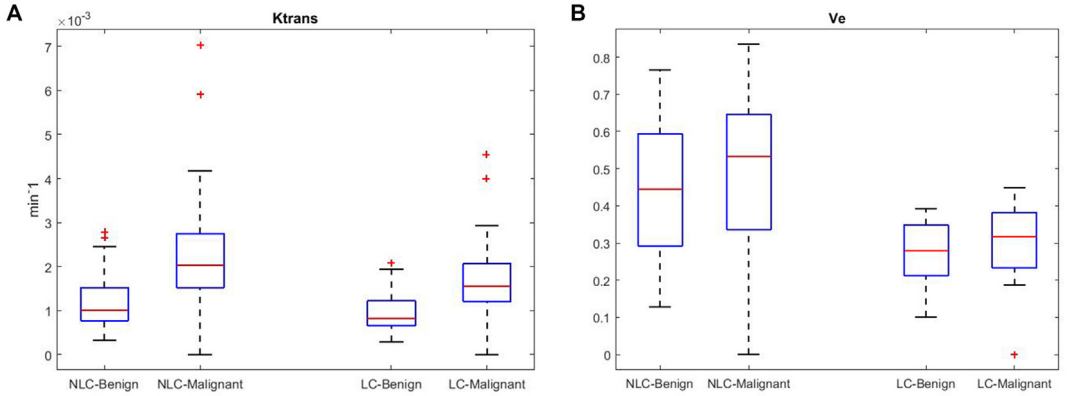

Fig. 5. (A) Estimated K^{trans} and (B) v_e values using NLC and LC for 10 patients with breast lesions.

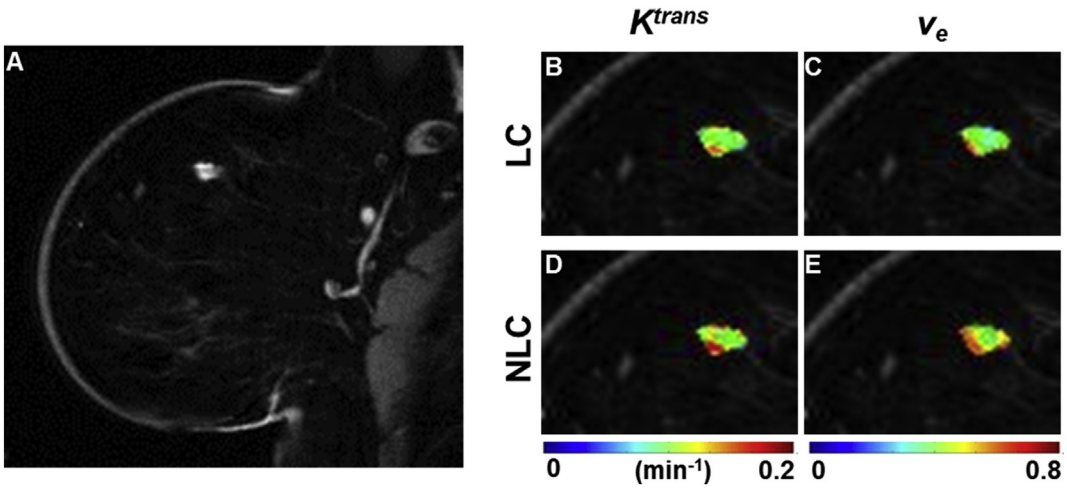

Fig. 6. Parametric Maps for (A) one representative subject with breast cancer. (B) LC K^{trans} and (C) LC v_e. (D) NLC K^{trans} and (E) NLC v_e.

accuracy of the LC method decreased dramatically as the FA decreased. These findings are similar to those by Guo et al. [32], who found that, for a spoiled gradient echo pulse sequence, the relationship between the relaxation rate change and signal enhancement is strongly non-linear for small FAs and approximately linear for large FAs. While a high FA may provide more accurate kinetic parameter estimates using the LC method [21], high FAs are not routinely used in DCE-MRI as they are less sensitive to the T_1 changes due to contrast injection [21,26,33,34]. In contrast, low FAs with the LC method are prone to error and consequently they are more disposed to concentration uncertainty [35]. Hence, it would be preferred to use an intermediate FA, such as 45°, in order to balance between the accuracy in parameter estimation and the sensitivity to contrast enhancement.

In regards to the T_{10} dependence on the estimation of K^{trans} and v_e, we found that there was substantial dependence of T_{10} in estimated K^{trans} and v_e using both LC and NLC methods. The LC method overestimated K^{trans} and v_e under all conditions. The NLC method provided accurate estimates when the correct T_{10} was assumed, but inaccurate estimates for all other conditions. In a similar study using rats, Heilmann et al. [20] found that the assumption of signal linearity resulted in K_{ep} values up to 60% higher than those measured using the NLC approach. Similarly, Guo et al. [32] demonstrated that K^{trans} is highly dependent on T_{10} and it approaches the true values only when T_{10} is close to the true T_{10} value. In our simulations, the T_{10} effect could not be ignored, even at FA = 45°. In cases where the T_{10} is not known, we found that using the LC method with a pAIF had lower T_{10} dependency of K^{trans} and v_e than other ways, including using the NLC method.

In order to compare the effect of using the two conversion methods on diagnostic performance, we assessed breast DCE-MRI data from 32 women and FA = 12°. We found that K^{trans} and v_e estimated using the LC method with pAIF were lower than those estimated using the NLC methods with the same AIF. In spite of this, the difference between the mean K^{trans} values of malignant and benign lesions, normalized by the standard deviation, was similar between the LC and NLC methods using the pAIF, in which both K^{trans} and v_e were underestimated with the LC method, which suggests that the findings from the present simulation study may apply to clinical data analysis in general. In clinical DCE-MRI studies, it is important to assess the reproducibility of measurements in order to evaluate changes in treatment response and to improve the specificity of DCE-MRI for cancer detection. However, most DCE-MRI studies are based on the routine clinical data in which T_{10} measurement is not available and the FA is substantially smaller than 45°. In such cases with clinical data, our results suggest that using the LC method with a population-based AIF may minimize the influence of T_1 differences between lesions or measurements, although K^{trans} would be likely underestimated as shown in Figs. 3 and 4. Such underestimation of K^{trans} reduces the dynamic range of K^{trans} which may or may not be acceptable depending on the needs in specific applications. Further studies are warranted to investigate if this same pattern holds true when using DCE-MRI and also to assess the pros and cons of using different analysis methods considered in this study in terms of differentiating lesions and assessing treatment efficacy.

The breast DCE-MRI data used in this study were acquired using the GRASP method [31]. GRASP provides a high temporal resolution, without compromising the spatial resolution that is required for quantitative contrast kinetic analyses. The GRASP image reconstruction is performed by minimizing both data consistency and the sparsity constraint. Total variation along the temporal dimension is used as the sparsity constraint which regularizes the dynamic data and allows to achieve good image quality and temporal fidelity [30]. While this type of compressed sensing image reconstruction method provides images with substantially reduced noise, they are not free of noise. However, the noise characteristics of these images from a non-linear image reconstruction, such as GRASP, are not well known and can vary depending on various factors, such as the type of sparsity constraint and the parameter estimation method. The assumption of Rician noise used in our simulation study may not be applicable to the breast DCE-MRI data. Hence, caution needs to be taken in comparing the simulation study results and that from the breast GRASP DCE-MRI data. Our study assessed the effect of T_{10} and FA, under the presence of noise, on the LC and NLC methods. The assumption on T_{10} and the choice of FA can introduce biases in the estimated parameters, whereas noise contributes more to the precision. Thus, we expect that the bias from assumed T_{10} values and FA would be similar in both simulation and GRASP data. But the precision found in the simulation study may not be applicable to the data analysis result with the GRASP data. Further study is needed to investigate the noise characteristics of advanced non-linear image reconstruction methods and its influence on estimation of contrast kinetic model parameters.

There are other limitations to our study. First, our study was conducted with the simplest contrast kinetic model; other contrast kinetic models including the extended Tofts model [36], the Brix model [37], the shutter-speed model [38], and the reference region model [39] were not evaluated. Particularly, contrast kinetic models including the water exchange effect, such as the shutter-speed model, can be very sensitive to estimation of T_1 values of tissue after contrast injection, which requires accurate measurement of T_{10}. It has not been shown whether the LC method itself can increase or decrease the sensitivity of DCE-MRI data to the water exchange effect. However, the requirement to use a higher FA for the LC method would make the T_1-weighted DCE-MRI data less sensitive to the water exchange effect [40] and may allow to

estimate the perfusion parameters without the need to incorporate the water exchange effect. Next, this study did not include the influence of other scan conditions including scan duration and could be extended to investigate the effect of other parameters in order to optimize the scan protocol in future simulations. Another limitation was that we used only one noise level. An increased noise level will reduce the precision. However, we expect that the overall trends that we observed in this study would not change with a higher level of noise. This study was conducted with one type of pAIF and one temporal resolution, although we expect that using other pAIF models and temporal resolutions would have shown similar results. Finally, our model was also tested in one type of cancer.

Future studies are necessary to compare the LC and NLC methods with more clinical data from different sites such that it can be assessed whether the LC-based kinetic parameters can be used to combine data from multiple sites without T_1 measurement. In addition, development of a statistical estimation tool to predict the uncertainty associated with each factor would be needed to have broad utility in studies with different practical limitations and to guide study design of future clinical DCE-MRI studies. An uncertainty estimation technique based on multivariate linear error propagation can be used to calculate uncertainty maps of pharmacokinetic parameters from the uncertainty in the input data as demonstrated by Garpebring et al. in 2013 when the NLC method is used [41]. It was also reported by Schabel and Parker that the uncertainty and bias in concentration measurement in the NLC can be minimized by selecting an optimal FA through their uncertainty and sensitivity analysis [35]. As demonstrated by these methods, more formal statistical estimation tools could be used to compare the expected uncertainty and bias of the contrast kinetic parameters with the LC and the NLC methods, which are needed to find the optimal data acquisition and analysis methods in practice for future quantitative DCE-MRI studies.

5. Conclusion

In this study, we have shown through both simulations and in vivo experiments that the LC and NLC approaches can provide different estimates of the contrast kinetic parameters K^{trans} and v_e. LC may provide more accurate parameter estimates when T_{10} is unknown, whereas NLC is able to provide more accurate robustness in kinetic parameter estimation, in particular in situations such as low FAs. The present study results also suggest that, when T_{10} is not measured and a low FA is used as in routine clinical DCE-MRI exam, the LC method with pAIF could be used to minimize the uncertainty introduced by an assumed T_{10}.

References

[1] Sourbron S, Ingrisch M, Siefert A, et al. Quantification of cerebral blood flow, cerebral blood volume, and blood-brain-barrier leakage with DCE-MRI. Magn Reson Med 2009;62:205–17.

[2] Kim S, Loevner LA, Quon H, et al. Prediction of response to chemoradiation therapy in squamous cell carcinomas of the head and neck using dynamic contrast-enhanced MR imaging. AJNR Am J Neuroradiol 2010;31:262–8.

[3] Turnbull LW. Dynamic contrast-enhanced MRI in the diagnosis and management of breast cancer. NMR Biomed 2009;22:28–39.

[4] Huang W, Li X, Morris EA, et al. The magnetic resonance shutter speed discriminates vascular properties of malignant and benign breast tumors in vivo. Proc Natl Acad Sci U S A 2008;105:17943–8.

[5] El Khouli RH, Macura KJ, Jacobs MA, et al. Dynamic contrast-enhanced MRI of the breast: quantitative method for kinetic curve type assessment. AJR Am J Roentgenol 2009;193:W295–300.

[6] Taouli B, Johnson RS, Hajdu CH, et al. Hepatocellular carcinoma: perfusion quantification with dynamic contrast-enhanced MRI. AJR Am J Roentgenol 2013;201:795–800.

[7] Flaherty KT, Rosen MA, Heitjan DF, et al. Pilot study of DCE-MRI to predict progression-free survival with sorafenib therapy in renal cell carcinoma. Cancer Biol Ther 2008;7:496–501.

[8] Chandarana H, Amarosa A, Huang WC, et al. High temporal resolution 3D gadolinium-enhanced dynamic MR imaging of renal tumors with pharmacokinetic modeling: preliminary observations. J Magn Reson Imaging 2013;38:802–8.

[9] Li L, Wang K, Sun X, et al. Parameters of dynamic contrast-enhanced MRI as imaging markers for angiogenesis and proliferation in human breast cancer. Med Sci Monit 2015;21:376–82.

[10] Hotker AM, Mazaheri Y, Aras O, et al. Assessment of prostate cancer aggressiveness by use of the combination of quantitative DWI and dynamic contrast-enhanced MRI. AJR Am J Roentgenol 2016;206:756–63.

[11] Whisenant JG, Sorace AG, McIntyre JO, et al. Evaluating treatment response using DW-MRI and DCE-MRI in trastuzumab responsive and resistant HER2-overexpressing human breast cancer xenografts. Transl Oncol 2014;7:768–79.

[12] Leach MO, Brindle KM, Evelhoch JL, et al. The assessment of antiangiogenic and anti-vascular therapies in early-stage clinical trials using magnetic resonance imaging: issues and recommendations. Br J Cancer 2005;92:1599–610.

[13] Tofts PS, Brix G, Buckley DL, et al. Estimating kinetic parameters from dynamic contrast-enhanced T(1)-weighted MRI of a diffusable tracer: standardized quantities and symbols. J Magn Reson Imaging 1999;10:223–32.

[14] Donahue KM, Weisskoff RM, Burstein D. Water diffusion and exchange as they influence contrast enhancement. J Magn Reson Imaging 1997;7:102–10.

[15] Materne R, Smith AM, Peeters F, et al. Assessment of hepatic perfusion parameters with dynamic MRI. Magn Reson Med 2002;47:135–42.

[16] Hittmair K, Gomiscek G, Langenberger K, et al. Method for the quantitative assessment of contrast agent uptake in dynamic contrast-enhanced MRI. Magn Reson Med 1994;31:567–71.

[17] Ronot M, Asselah T, Paradis V, et al. Liver fibrosis in chronic hepatitis C virus infection: differentiating minimal from intermediate fibrosis with perfusion CT. Radiology 2010;256:135–42.

[18] Materne R, Van Beers BE, Smith AM, et al. Non-invasive quantification of liver perfusion with dynamic computed tomography and a dual-input one-compartmental model. Clin Sci 2000;99:517–25.

[19] Van Beers BE, Materne R, Annet L, et al. Capillarization of the sinusoids in liver fibrosis: noninvasive assessment with contrast-enhanced MRI in the rabbit. Magn Reson Med 2003;49:692–9.

[20] Heilmann M, Kiessling F, Enderlin M, Schad LR. Determination of pharmacokinetic parameters in DCE MRI: consequence of nonlinearity between contrast agent concentration and signal intensity. Investig Radiol 2006;41:536–43.

[21] Aronhime S, Calcagno C, Jajamovich GH, et al. DCE-MRI of the liver: effect of linear and nonlinear conversions on hepatic perfusion quantification and reproducibility. J Magn Reson Imaging 2014;40:90–8.

[22] Sourbron S, Sommer WH, Reiser MF, Zech CJ. Combined quantification of liver perfusion and function with dynamic gadoxetic acid-enhanced MR imaging. Radiology 2012;263:874–83.

[23] Koh TS, Thng CH, Lee PS, et al. Hepatic metastases: in vivo assessment of perfusion parameters at dynamic contrast-enhanced MR imaging with dual-input two-compartment tracer kinetics model. Radiology 2008;249:307–20.

[24] Nelder JA, MR. A simplex method for function minimization. Comput J 1965;7:308–13.

[25] Parker GJ, Roberts C, Macdonald A, et al. Experimentally-derived functional form for a population-averaged high-temporal-resolution arterial input function for dynamic contrast-enhanced MRI. Magn Reson Med 2006;56:993–1000.

[26] El Khouli RH, Macura KJ, Kamel IR, et al. 3-T dynamic contrast-enhanced MRI of the breast: pharmacokinetic parameters versus conventional kinetic curve analysis. AJR Am J Roentgenol 2011;197:1498–505.

[27] Kim SG, Freed M, Leite AP, et al. Separation of benign and malignant breast lesions using dynamic contrast enhanced MRI in a biopsy cohort. J Magn Reson Imaging 2017;45(5):1385–93.

[28] de Bazelaire CM, Duhamel GD, Rofsky NM, Alsop DC. MR imaging relaxation times of abdominal and pelvic tissues measured in vivo at 3.0 T: preliminary results. Radiology 2004;230:652–9.

[29] Lu H, Clingman C, Golay X, van Zijl PC. Determining the longitudinal relaxation time (T1) of blood at 3.0 Tesla. Magn Reson Med 2004;52:679–82.

[30] Kim SG, Feng L, Grimm R, et al. Influence of temporal regularization and radial undersampling factor on compressed sensing reconstruction in dynamic contrast enhanced MRI of the breast. J Magn Reson Imaging 2016;43:261–9.

[31] Feng L, Grimm R, Block KT, et al. Golden-angle radial sparse parallel MRI: combination of compressed sensing, parallel imaging, and golden-angle radial sampling for fast and flexible dynamic volumetric MRI. Magn Reson Med 2014;72:707–17.

[32] Guo JY, Reddick WE, Rosen MA, Song HK. Dynamic contrast-enhanced magnetic resonance imaging parameters independent of baseline T10 values. Magn Reson Imaging 2009;27:1208–15.

[33] Batchelor TT, Sorensen AG, di Tomaso E, et al. AZD2171, a pan-VEGF receptor tyrosine kinase inhibitor, normalizes tumor vasculature and alleviates edema in glioblastoma patients. Cancer Cell 2007;11:83–95.

[34] Schwenzer NF, Kotter I, Henes JC, et al. The role of dynamic contrast-enhanced MRI in the differential diagnosis of psoriatic and rheumatoid arthritis. AJR Am J Roentgenol 2010;194:715–20.

[35] Schabel MC, Parker DL. Uncertainty and bias in contrast concentration measurements using spoiled gradient echo pulse sequences. Phys Med Biol 2008;53:2345–73.

[36] Tofts PS. Modeling tracer kinetics in dynamic Gd-DTPA MR imaging. J Magn Reson Imaging 1997;7:91–101.

[37] Brix G, Kiessling F, Lucht R, et al. Microcirculation and microvasculature in breast tumors: pharmacokinetic analysis of dynamic MR image series. Magn Reson Med 2004;52:420–9.

[38] Yankeelov TE, Rooney WD, Li X, Springer Jr. CS. Variation of the relaxographic "shutter-speed" for transcytolemmal water exchange affects the CR bolus-tracking curve shape. Magn Reson Med 2003;50:1151–69.

[39] Yankeelov TE, Luci JJ, Lepage M, et al. Quantitative pharmacokinetic analysis of DCE-MRI data without an arterial input function: a reference region model. Magn Reson Imaging 2005;23:519–29.

[40] Zhang J, Kim S. Uncertainty in MR tracer kinetic parameters and water exchange rates estimated from T1-weighted dynamic contrast enhanced MRI. Magn Reson Med 2014;72:534–45.

[41] Garpebring A, Brynolfsson P, Yu J, et al. Uncertainty estimation in dynamic contrast-enhanced MRI. Magn Reson Med 2013;69:992–1002.